

COMMUNICATIONS

Predissociation dynamics of formyloxyl radical studied by the dissociative photodetachment of $\text{HCO}_2^-/\text{DCO}_2^- + h\nu \rightarrow \text{H/D} + \text{CO}_2 + e^-$

Todd G. Clements and Robert E. Continetti

Department of Chemistry and Biochemistry, University of California, San Diego, 9500 Gilman Drive, La Jolla, California 92093-0340

(Received 15 June 2001; accepted 27 July 2001)

The dissociative photodetachment (DPD) of HCO_2^- and DCO_2^- was studied at 258 nm. State-resolved translational energy distributions were observed correlated to bending excitation in the CO_2 product for the channel producing $\text{H/D} + \text{CO}_2$, indicating very low rotational excitation in the products consistent with predissociation of a C_{2v} HCO_2 molecule. No evidence was found for dissociation into $\text{OH} + \text{CO}$. All three low-lying electronic states (2A_1 , 2B_2 , and 2A_2) were found to dissociate, but resolved progressions were only observed from photodetachment to the 2A_1 and 2B_2 states. Photoelectron-photofragment coincidence spectra for DCO_2^- show resolved vertical bands and indicate that multiple CO_2 vibrational states are accessible from each vibrational level in the predissociating DCO_2 molecule. The resolved structure is assigned to vibrational predissociation sequence bands, observable in this DPD process owing to the dissociation dynamics and the near degeneracy of the vibrational levels in the 2A_1 and 2B_2 states of HCO_2 and the bending mode of the CO_2 products. © 2001 American Institute of Physics. [DOI: 10.1063/1.1404143]

The formyloxyl radical, HCO_2 , has attracted experimental and theoretical attention owing to its role as a possible intermediate in the $\text{H} + \text{CO}_2 \rightarrow \text{OH} + \text{CO}$ reaction, of interest both in combustion and atmospheric chemistry.¹⁻³ The dynamics of this bimolecular reaction have been explored experimentally through the use of hot atom collisions, which yield state resolved distributions for inelastic collisions with the CO_2 molecule⁴ or for the OH reaction products.^{5,6} Photodissociation of van der Waals precursors such as the XH-OCO ($\text{X} = \text{Br}, \text{I}$) complex have also been employed in order to study dynamics through an HOCO intermediate.^{7,8} The electronic structure of HCO_2 is a challenging theoretical problem owing to two low-lying excited states that can mix strongly and lead to symmetry breaking from a C_{2v} geometry.⁹⁻¹² The interest in this system has also prompted the calculation of a potential energy surface by Schatz and co-workers for use in dynamics studies of the $\text{H} + \text{CO}_2 \rightarrow \text{OH} + \text{CO}$ reaction.^{1,13,14}

The HCO_2 radical itself has proven difficult to observe experimentally.^{15,16} In order to study the energetics and structure of HCO_2 and DCO_2 , Neumark and co-workers measured the photoelectron spectra of HCO_2^- and DCO_2^- , and observed vibrationally resolved progressions dominated by the CO_2 bend.¹⁶ They determined that H-CO_2 was energetically unstable relative to $\text{H} + \text{CO}_2$, however, the observation of sharp features in the photoelectron spectra showed that the nascent neutral was long lived with respect to the time scale of molecular vibrations. Thus these experiments characterized the metastable states of the radical, but provided no insight into the dissociation dynamics.

In the experiments reported here, dissociative photodetachment (DPD) of $\text{HCO}_2^-/\text{DCO}_2^-$ is used to probe the disso-

ciation dynamics of the transient formyloxyl radical. Photoelectron-photofragment coincidence (PPC) spectroscopy provides a method to study energy-selected neutral molecules by photodetachment of the corresponding anion. A coincidence measurement of the photoelectron and photofragment translational energy release characterizes the partitioning of energy among the products, yielding significant insight into the neutral dissociation dynamics.^{17,18}

The PPC spectrometer has been described in detail previously, and will only be briefly reviewed here.¹⁹ HCO_2^- was made by crossing a 1 keV electron beam with a continuous supersonic expansion of N_2O that had been passed over a formic acid solution. The anions were accelerated to 7 keV and re-referenced to ground by a high-voltage potential switch running at a 1 kHz repetition rate. Anions with $m/e = 45$ were mass selected by time-of-flight and intersected by the linearly polarized third harmonic (258 nm, 4.80 eV, 1.2 ps FWHM) of the regeneratively amplified output of a Ti:Sapphire laser (Clark CPA-2000). Photodetached electrons were detected by one of two opposed time- and position-sensitive electron detectors perpendicular to both the ion and laser beams. The time and position information is used to correct for the large Doppler shift arising from the fast ion beam. Using the photoelectron spectrum of I^- at 258 nm, the center-of-mass (CM) electron kinetic energy resolution (eKE) was determined to be $\Delta E/E \approx 7\%$ at 0.8 eV and 7 keV beam energy. Photofragments recoiled out of the beam along a 104 cm flight path and were detected with a multi-particle time- and position-sensitive detector. Conservation of momentum and the time and position information were employed to calculate the photofragment mass ratio and the CM kinetic energy release of the particles. The photodisso-

ciation of O_2^- at 258 nm was used to calibrate the detector, which showed a resolution of $\Delta E/E \approx 11\%$ at 0.70 eV translational energy (E_T) and 7 keV beam energy.

Owing to the small mass of the H or D product and consequently the large CM velocities, the angular acceptance of the detector is small. Monte Carlo simulations of the apparatus and dissociation dynamics were used to estimate the acceptance function of the detector. To approximate the actual translational energy distribution, $P(E_T)$, from the experimental distribution, $N(E_T)$, a large number of trajectories (5×10^6 for HCO_2^-) were run where each dissociation event had an equal $P(E_{T,MC})$ and an isotropic angular distribution from 0 to 2 eV. Those events where one particle landed outside of the detector region were discarded. The resultant $N(E_{T,MC})$ distribution was divided into the experimental $N(E_T)$ distribution to yield an approximate $P(E_T)$.²⁰ This correction significantly reduced the intensity of events below approximately 0.1 eV, and had little effect above 0.2 eV. Given the energetics and dynamics of the dissociations, the angular acceptance of the detector is approximately 8% of all dissociation events for HCO_2^- and 15% for DCO_2^- .

Figure 1 shows the $P(E_T)$ distributions for dissociation of HCO_2^- and DCO_2^- after photodetachment. All the data shown are for the pathway forming $\text{H} + \text{CO}_2$ as no evidence of stable products or dissociation into $\text{OH} + \text{CO}$ was found in the data. The dominant feature in both spectra is the progression that becomes resolved below approximately 0.6 eV in both HCO_2^- and DCO_2^- . Figure 2 shows the photoelectron-photofragment correlation spectrum for $\text{DCO}_2^- + h\nu \rightarrow \text{D} + \text{CO}_2 + e^-$. The two-dimensional image shows a histogram of the correlation between E_T and eKE for each event. The $N(E_T)$ and $N(\text{eKE})$ spectra are generated by integrating over the conjugate variable in the spectrum. The photoelectron spectrum is similar to that acquired by Neumark and co-workers, although the apparatus used in those experiments had better energy resolution, and resolved progres-

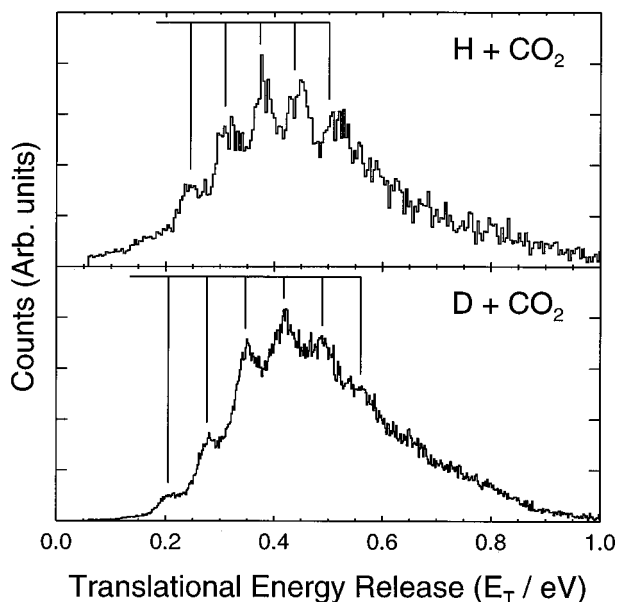


FIG. 1. The translational energy release distribution, $P(E_T)$, for the reaction $\text{HCO}_2^-/\text{DCO}_2^- + h\nu \rightarrow \text{H/D} + \text{CO}_2 + e^-$ at 258 nm.

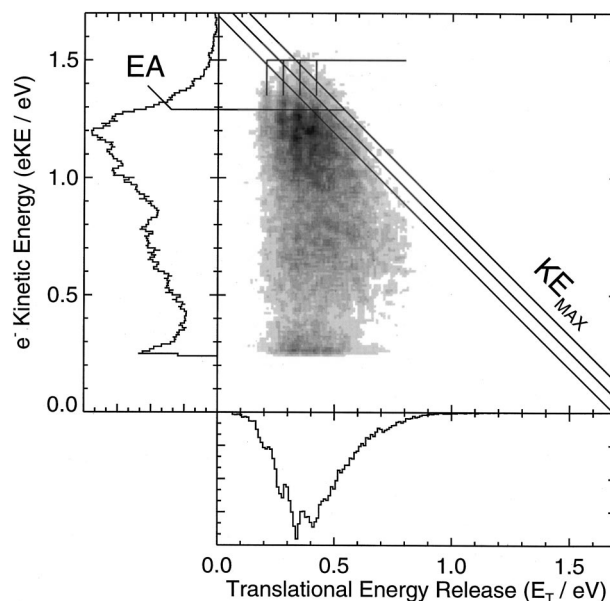


FIG. 2. Photoelectron-photofragment correlation spectrum, $N(E_T, \text{eKE})$, for the reaction $\text{DCO}_2^- + h\nu \rightarrow \text{D} + \text{CO}_2 + e^-$ at 258 nm. The rightmost diagonal line corresponds to the maximum translational energy release (KE_{max}) where the D and CO_2 products are in their ground internal and electronic states and the two lines to the left represent $\nu=1,2$ in the CO_2 product bending vibration. The electron affinity (Ref. 16) is also marked. The vertical lines highlight the predissociation sequence bands as discussed in the text.

sions were observed.¹⁶ No attempt was made in the correlation spectrum to correct for the acceptance function of the detector, but comparison of the $N(E_T)$ spectrum to that in Fig. 1 shows that this does not have a significant effect for DCO_2^- . The correlation spectrum shows vertical bands, spaced by the same amount as the peaks in the $\text{DCO}_2^- P(E_T)$ spectrum in Fig. 1.

In the photoelectron spectrum of CO_2^- , Bowen and co-workers observed a progression spaced by approximately 60 meV that they concluded to be most consistent with high excitation of the CO_2 bending mode.^{21,22} In this case, the spectrum was dominated by the large geometry change going from the bent anion ($\theta \approx 134^\circ$) to the linear neutral.²³⁻²⁵ The OCO bond angle in HCO_2^- is approximately 130° ,^{16,26,27} thus excitation of the CO_2 bending mode would be expected following dissociation of the C-H bond. The average peak spacing in the $P(E_T)$ spectra is 64 meV (520 cm^{-1}) in HCO_2^- and 71 meV (570 cm^{-1}) in DCO_2^- . These values are in between the 667.4 cm^{-1} literature value for the gas phase CO_2 bend,²⁸ and the 485 cm^{-1} spacing seen by Bowen and co-workers, implying a lower level of bending excitation than produced in the photodetachment of CO_2^- . The peak spacing is also similar to that assigned by Neumark *et al.* to the CO_2 bending mode (ω_3) in HCO_2^- (613 cm^{-1} for 2A_1 , 550 cm^{-1} for 2B_2) and DCO_2^- (620 cm^{-1} for 2A_1 , 530 cm^{-1} for 2B_2).¹⁶ Even though CO_2^- and HCO_2^- have similar OCO bond angles, lower bending excitation in the dissociation of HCO_2^- is consistent with some of the geometrical strain in the nascent neutral being released as translational energy. As discussed below, however, the structure in the $P(E_T)$ distribution must result not from individual CO_2 bending states, but

from a sequence band, arising from predissociation of different neutral states to different product states with the same translational energy release.

Neumark and co-workers estimated the bond dissociation energy, ΔD_0 , for $\text{H}-\text{CO}_2$ to be -0.58 ± 0.13 eV, showing that HCO_2 is energetically unstable relative to $\text{H}+\text{CO}_2$.¹⁶ Calculations at the QCISD/6-311++G**//MP2/6-311++G** level, using the GAUSSIAN 94 suite of programs,²⁹ show that the zero point energy of DCO_2 is reduced by 0.04 eV relative to HCO_2 . Assuming that cold anions are produced, subtracting the zero-point-corrected ΔD_0 and the electron affinity (EA) of DCO_2 (3.510 eV)¹⁶ from the photon energy (4.80 eV) yields a maximum translational energy of $KE_{\text{MAX}} = h\nu - \text{EA} - \Delta D_0 = 1.83$ eV when D and CO_2 are produced in their ground electronic and internal states. KE_{MAX} is marked as the rightmost diagonal line in Fig. 2. Data below KE_{MAX} imply rovibrational or electronic excitation in the products. The $N(E_T, eKE)$ spectrum reveals a series of vertical bands that correlate with the resolved features observed in the $P(E_T)$ spectrum. This structure differs from that observed in previous examples of DPD dynamics. In the O_4^- (Ref. 30) and O_6^- (Ref. 31) systems, diagonal ridges were seen corresponding to direct DPD on a series of vibrationally adiabatic curves correlating to ground electronic state O_2 in different vibrational levels. In the DPD of the excited electronic states of O_3^- (Ref. 32), the $N(E_T, eKE)$ spectrum revealed a series of horizontal bands corresponding to the product internal energy distribution for predissociation of specific states of the O_3 neutral.

The structured photoelectron spectrum observed by Neumark and co-workers shows that DPD of DCO_2^- also occurs by predissociation. The simplest explanation for the structure in the $N(E_T, eKE)$ spectrum is that each of the vertical bands represents a series of product CO_2 vibrational states produced from a series of nascent bend-excited states in HCO_2 , with a fixed change in bending quantum number between the predissociative state and the CO_2 product for each vertical band. In other words, we assign these features to predissociation sequence bands. Schematic potential energy surfaces which would lead to the observation of these bands are drawn in Fig. 3. For this structure to be observable, the repulsion between $\text{H}+\text{CO}_2$ upon reaching the dissociative state must be the same for each of the CO_2 bending states produced in a given band. This will occur for a fixed change in bending quantum number if the neutral and product state vibrational spacings are nearly degenerate and the dissociation dynamics are vibrationally adiabatic and lead to low rotational excitation. The distribution along the E_T direction shows that each of the bending states excited in DCO_2 can predissociate to a distribution of CO_2 product bending states. A qualitative assignment of the features near the marked EA ($eKE = 1.29$ eV) based on the energetic difference from KE_{MAX} shows correlation to $\nu = 2, 3, 4$, and 5 of the CO_2 product for the four clearly resolved bands. According to the assignment of the spectra by Neumark and co-workers, the signal in the photoelectron spectrum at this energy arises primarily from excitation to $\omega_3 = 0$ in the 2A_1 electronic state of DCO_2 .¹⁶ Excitation of higher vibrational levels of the DCO_2 intermediate (lower eKE) must yield

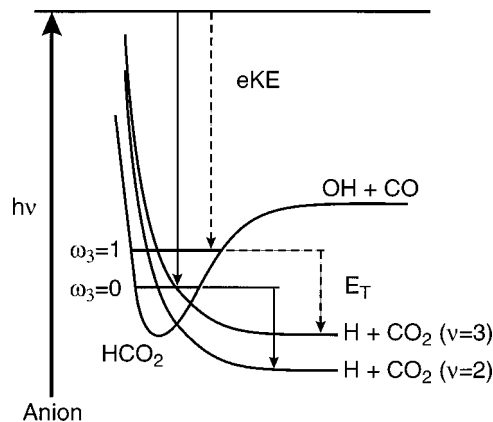


FIG. 3. Schematic potential energy surface illustrating the predissociation dynamics of HCO_2 . Excitation to $\omega_3 = 0$ of the HCO_2 radical followed by dissociation to $\text{H}+\text{CO}_2$ ($\nu = 2$) has characteristic electron and particle translational energies shown by the solid arrows. However, due to the near degeneracy between the HCO_2 and CO_2 vibrational spacings, excitation to $\omega_3 = 1$ of the HCO_2 radical followed by dissociation to $\text{H}+\text{CO}_2$ ($\nu = 3$), shown by the dashed arrows, has the same E_T , but lower eKE, resulting in the vibrational predissociation sequence bands seen in Fig. 2.

higher levels of CO_2 product excitation to maintain the vertical structure. Data at higher electron energy resolution would yield a vertically spaced series of peaks, instead of bands, where both the initial product state and final product state could be uniquely identified.

The structure in the $N(E_T, eKE)$ spectrum is observed in both the 2A_1 and 2B_2 states, but is not seen for excitation to the 2A_2 state. A possible explanation arises from examination of the potential energy surfaces of the three participating electronic states. Theoretical studies have predicted a conical intersection between the 2B_2 and the 2A_1 electronic states of HCO_2 at OCO angles between 125° and 135° .^{10-12,33-35} Photodetachment from the anion, where the OCO angle is near 130° ,^{16,26,27} accesses the region of the potential surface near the intersection between the 2B_2 and the 2A_1 states. Since only the 2A_1 state correlates directly to ground state $\text{H}+\text{CO}_2$ and excitation to the 2B_2 state results in the same product vibrational distribution, it is likely that the 2B_2 state is accessing the conical intersection and dissociates through the 2A_1 state. The vibrational distribution of the products is thus only dependent on the exit channel from the 2A_1 state, and not on the initial state excited.

The 2A_2 state is also dissociative, but does not produce the distinct vertical structure seen for the 2B_2 and 2A_1 states. Closer examination of this region of the correlation spectrum reveals a broad $N(E_T)$ distribution with only barely resolved vibrational peaks. Feller *et al.*³⁵ and Peyerimhoff *et al.*³³ proposed that the 2A_2 state intersects the 2A_1 state higher on the repulsive curve (smaller OCO angle) than the 2B_2 state. In this case, the crossing between these two curves provides a radiationless route to ground state $\text{H}+\text{CO}_2$ and should increase the average E_T of the products as can be seen upon careful inspection of the correlation spectrum. The increased energy may also partition into combination bands or rotation due to the greater molecular distortion at the point of curve crossing, which would broaden the spectra and reduce the apparent correlation, as seen in the data. In fact, Neumark

and co-workers noted that combination bands contribute significantly to spectrum of the 2A_2 state of HCO_2 and DCO_2 .¹⁶

In conclusion, the DPD of HCO_2^- and DCO_2^- is found to exhibit dissociation dynamics consistent with predissociation to $\text{H}+\text{CO}_2$ products from the three lowest-lying states of HCO_2 . Photodetachment to the 2A_1 and 2B_2 states leads to characteristic dynamics where each predissociated vibrational state of HCO_2 produces several CO_2 product vibrational states with low rotational excitation. Furthermore, owing to the near degeneracy of the O–C–O bending excitation in HCO_2 and the $\text{H}+\text{CO}_2$ products, predissociations connecting pairs of HCO_2 and CO_2 product bending states with the same energy difference appear at a nearly constant product E_T , leading to the observation of vertical bands in the $N(E_T, e\text{KE})$ spectra. The 2A_2 state of HCO_2 and DCO_2 was also dissociative but did not show state-resolved $N(E_T)$ distributions, indicating that predissociation of this electronic state occurs with more distortion of the C_{2v} framework and involves other vibrational modes. This experiment provides the first information on the dissociation dynamics of the transient HCO_2 radical. The striking state-resolved vibrational predissociation sequence bands observed will provide an important test for potential energy surfaces and dynamics calculations on this transient species.

This work was supported by the Department of Energy (DOE) under Grant No. DE-FG03-98ER14879. One of the authors (T.G.C.) is supported under AFOSR Grant No. F49620-000-10-010. One of the authors (R.E.C.) is a Camille Dreyfus Teacher-Scholar and a Packard Fellow in Science and Engineering.

¹K. Kudla, G. C. Schatz, and A. F. Wagner, *J. Chem. Phys.* **95**, 1635 (1991).

²C. Wittig, S. Sharpe, and R. A. Beaudet, *Acc. Chem. Res.* **21**, 341 (1988).

³D. Fulle, H. F. Hamann, H. Hippler, and J. Troe, *J. Chem. Phys.* **105**, 983 (1996).

⁴G. W. Flynn and R. E. Weston, Jr., *J. Phys. Chem.* **97**, 8116 (1993).

⁵M. Brouard, D. W. Hughes, K. S. Kalogerakis, and J. P. Simons, *J. Phys. Chem. A* **102**, 9559 (1998).

⁶M. Brouard, D. W. Hughes, K. S. Kalogerakis, and J. P. Simons, *J. Chem. Phys.* **112**, 4557 (2000).

⁷G. Hoffmann, D. Oh, Y. Chen, Y. M. Engel, and C. Wittig, *Isr. J. Chem.* **30**, 115 (1990).

⁸S. K. Shin, C. Wittig, and W. A. Goddard, *J. Phys. Chem.* **95**, 8048 (1991).

⁹A. D. McLean, B. H. Lengsfeld III, J. Pacansky, and Y. Ellinger, *J. Chem. Phys.* **83**, 3567 (1985).

¹⁰A. Rauk, D. Yu, and D. A. Armstrong, *J. Am. Chem. Soc.* **116**, 8222 (1994).

¹¹J. F. Stanton and N. S. Kadagathur, *J. Mol. Struct.* **376**, 469 (1996).

¹²P. Y. Ayala and H. B. Schlegel, *J. Chem. Phys.* **108**, 7560 (1998).

¹³D. C. Clary and G. C. Schatz, *J. Chem. Phys.* **99**, 4578 (1993).

¹⁴K. S. Bradley and G. C. Schatz, *J. Chem. Phys.* **106**, 8464 (1997).

¹⁵B. Ruscic, M. Schwarz, and J. Berkowitz, *J. Chem. Phys.* **91**, 6780 (1989).

¹⁶E. H. Kim, S. E. Bradforth, D. W. Arnold, R. B. Metz, and D. M. Neumark, *J. Chem. Phys.* **103**, 7801 (1995).

¹⁷R. E. Continetti, *Int. Rev. Phys. Chem.* **17**, 227 (1998).

¹⁸H.-J. Deyerl, A. K. Luong, T. G. Clements, and R. E. Continetti, *Faraday Discuss.* **115**, 147 (2000).

¹⁹K. A. Hanold, A. K. Luong, T. G. Clements, and R. E. Continetti, *Rev. Sci. Instrum.* **70**, 2268 (1999).

²⁰C. R. Sherwood and R. E. Continetti, *Chem. Phys. Lett.* **258**, 171 (1996).

²¹K. H. Bowen and J. G. Eaton, in *The Structure of Small Molecules and Ions*, edited by R. Naaman and Z. Vager (Plenum, New York, 1988), p. 147.

²²J. V. Coe, Ph.D. Thesis, The Johns Hopkins University, 1986.

²³J. F. Paulson, *J. Chem. Phys.* **22**, 963 (1970).

²⁴R. N. Compton, P. W. Reinhardt, and C. D. Cooper, *J. Chem. Phys.* **63**, 3821 (1975).

²⁵S. V. Krishna Kumar and V. S. Venkatasubramanian, *J. Chem. Phys.* **79**, 6423 (1983).

²⁶W. H. Zachariasen, *J. Am. Chem. Soc.* **92**, 1011 (1940).

²⁷M. Masamura, *Theor. Chim. Acta* **75**, 433 (1989).

²⁸G. Herzberg, *Molecular Spectra and Molecular Structure III. Electronic Spectra and Electronic Structure of Polyatomic Molecules* (Krieger Publishing, Malabar, 1991).

²⁹M. J. Frisch, G. W. Trucks, H. B. Schlegel *et al.*, GAUSSIAN 94, Revision E.2 (Gaussian, Inc., Pittsburgh, PA, 1995).

³⁰K. A. Hanold and R. E. Continetti, *Chem. Phys.* **239**, 493 (1998).

³¹K. A. Hanold, A. K. Luong, and R. E. Continetti, *J. Chem. Phys.* **109**, 9215 (1998).

³²M. C. Garner, K. A. Hanold, M. S. Resat, and R. E. Continetti, *J. Phys. Chem. A* **101**, 6577 (1997).

³³S. D. Peyerimhoff, P. S. Skell, D. D. May, and R. J. Buenker, *J. Am. Chem. Soc.* **104**, 4515 (1982).

³⁴A. Rauk, D. Yu, P. Borowski, and B. Roos, *Chem. Phys.* **197**, 73 (1995).

³⁵D. Feller, E. S. Huyser, W. T. Borden, and E. R. Davidson, *J. Am. Chem. Soc.* **105**, 1459 (1983).